Copyright © 2014 IEEE. Personal use of this material is permitted. Permission from IEEE must be obtained for all other uses, in any current or future media, including reprinting/republishing this material for advertising or promotional purposes, creating new collective works, for resale or redistribution to servers or lists, or reuse of any copyrighted component of this work in other works.

Contributions of Single–Phase Rooftop PVs on Short Circuits Faults in Residential Feeders

Hadi Hosseinian Yengejeh, Farhad Shahnia and Syed M. Islam
Electrical and Computer Engineering Department
Curtin University
Perth, Australia
hadi.hosseinian@postgrad.curtin.edu.au

***Abstract*—Sensitivity analysis results are presented to investigate the presence of single–phase rooftop Photovoltaic Cells (PV) in low voltage residential feeders, during short circuits in the overhead lines. The PV rating and location in the feeder and the fault location are considered as the variables of the sensitivity analysis. The single–phase faults are the main focus of this paper and the PV effect on fault current, current in distribution transformer secondary and the voltage at each bus of the feeder are investigated, during fault. Furthermore, to analyze the bus voltages and fault current in the presence of multiple PVs, each with different rating and location, a stochastic analysis is carried out to investigate the expected probability density function of these parameters, considering the uncertainties of PV rating and location as well as fault location.**

***Index Terms*—Rooftop PVs, Short circuit, Protection system**

I. Introduction

Rooftop Photovoltaic cells, (referred as PVs in this paper) are one of most common type of the renewable energy resources currently available in residential Low Voltage (LV) networks. Several researches have investigated the power quality problems due to high penetration of renewable resources and specifically the rooftop PVs in distribution networks such as voltage rise and voltage unbalance [1–3] and some improvement methods are already proposed to address these drawbacks [4–5].

Residential LV distribution feeders in suburban areas are traditionally radial and the existing protection schemes are designed to protect them based on their radial structure and unidirectional power flow assumption. High penetration of rooftop PVs in these feeders modifies the unidirectional power flow and affects the fault current and its direction.

The impacts of three–phase PV plants installed in Medium Voltage (MV) distribution systems are already investigated in [6–7] and it is proved that it depends on the generation capacity, installation point and availability of the PV plants in the network and the network demand level [8]. In [9–10] it is shown that installation of three–phase renewable energy resources in MV networks will lead miscoordination among protection devices, unwanted tripping, protection blinding and asynchronous reclosing. In [6,11–13] it is discussed that higher penetration of three–phase renewable resources requires some changes in the traditional protection schemes such as applying bidirectional relays, communication based transfer trips, pilot signal relaying, and impedance–based fault–protection schemes. Ref. [14] has proposed that MV network can be divided to several zones and each zone is separated from the others by reclosers and controllable circuit breakers. Ref. [15] proposed the application of an adaptive distance protection to consider the changes of output power of the renewable energy resources.

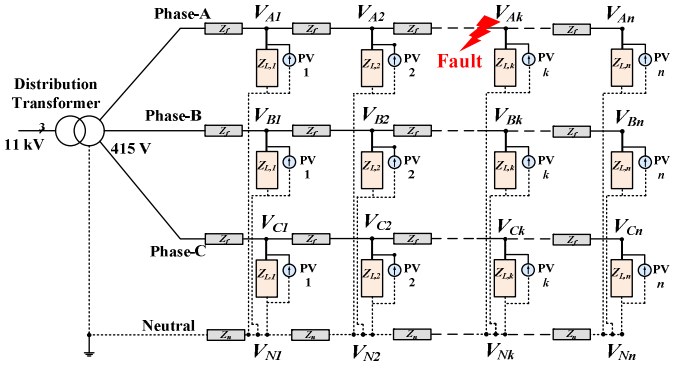

Fig. 1. Network under consideration.

However, no extensive research is carried out on the contribution of single–phase PVs, installed in LV feeders, on the fault current and performance of the protection devices. The two important factors which differentiate the residential PVs from other types of renewable resources are their single–phase connection and converter–interfaced structure [16]. Only in [17], the contribution of PVs in fault current is investigated but the fault is only considered at distribution boxes and not the overhead lines that are more vulnerable to faults.

In this paper, the contribution of rooftop PVs are investigated on the fault current as well as the voltage, present across the loads and PVs in the network, during a single–phase to ground fault in the LV overhead lines. Sensitivity and stochastic analyses are carried out in MATLAB to consider the effect of PVs and sample results are validated by time–domain simulations in PSCAD/EMTDC.

II. Network Structure and Modelling

Let us consider an 11 kV MV feeder, supplying a 100 kVA three–phase, 11kV/415 V, Dyn distribution transformer (Fig. 1). The transformer is supplying a residential network through a 3–phase 4–wire overhead line. Each phase and neutral conductor has a length of 400 m, spread over 10 poles (bus), with equal distance of 40 m from each other. The LV feeder is supplying 30 houses, distributed equally among the

three phases (i.e. 1 house per phase per pole). The PVs are assumed to be single–phase and converter–interfaced, running at unity power factor.

A. Network Generalized Model

First, it is required to derive a generalized network model to be utilized in the short circuit calculations. As the PVs are distributed unequally among the three phases and at different buses along each phase, the network always has an asymmetric configuration. This is valid regardless of the fault type. Therefore, it is required that the equivalent sequence network to be calculated. Assuming an equivalent distance between two adjacent buses in the LV feeder, the impedance matrix is represented as

$$[\boldsymbol{Z}_f^{LV}]_{ABC} = z_f.\boldsymbol{I}(3,3) \tag{1}$$

where z_f is equal to the impedance of one phase between two adjacent buses and $\boldsymbol{I}(3,3)$ is the identity matrix. Similarly, the MV feeder impedance is represented as

$$[\boldsymbol{Z}_f^{MV}]_{ABC} = z'_f.\boldsymbol{I}(3,3) \tag{2}$$

where z'_f is equal to the impedance of one phase of the MV feeder. The impedance of the distribution transformer can also be shown as

$$[\boldsymbol{Z}^{trans}]_{ABC} = z_{trans}.\boldsymbol{I}(3,3) \tag{3}$$

where z_{trans} is the equivalent per–phase impedance of the distribution transformer.

From (1), the feeder impedance in sequence components is defined as

$$[\boldsymbol{Z}_f^{LV}]_{012} = [\boldsymbol{A}]^{-1}[\boldsymbol{Z}_f^{LV}]_{ABC}[\boldsymbol{A}] \tag{4}$$

$$\text{where } [\boldsymbol{A}] = \begin{bmatrix} 1 & 1 & 1 \\ 1 & a^2 & a \\ 1 & a & a^2 \end{bmatrix} \text{ and } a = 1\angle 120°$$

Similarly, the sequence components for the MV feeder and transformer impedance are calculated from (2)–(3).

Let us assume the matrix of the output current of PVs connected to phase–A, B and C at bus i ($1 \le i \le n$) is given as

$$[\boldsymbol{I}_i^{PV}] = [I_A^{PV} \quad I_B^{PV} \quad I_C^{PV}]_i^T \tag{5}$$

where T is the transpose operator. From (5), the output current of PVs in each bus in sequence components is defined as

$$[\boldsymbol{I}_i^{PV}]_{012} = [\boldsymbol{A}]^{-1}[\boldsymbol{I}_i^{PV}]_{ABC} \tag{6}$$

From (4) and (6), for an asymmetrical fault at bus k of the network of Fig. 1, the equivalent sequence networks is modelled as shown in Fig. 2. The network is later required to be simplified using the Thevenin–Norton equivalent circuit from the fault point of view. This simplification is carried out separately for the PVs available in the downstream and upstream of the fault location. For the downstream PVs, their output currents are summed, based on Norton equivalent circuit as

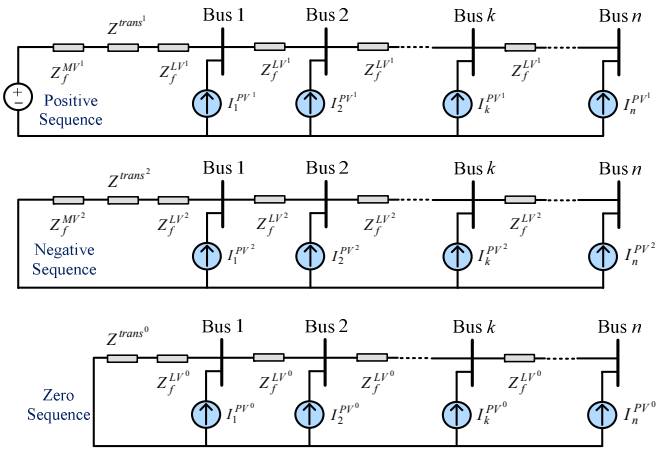

Fig. 2. Equivalent sequence networks.

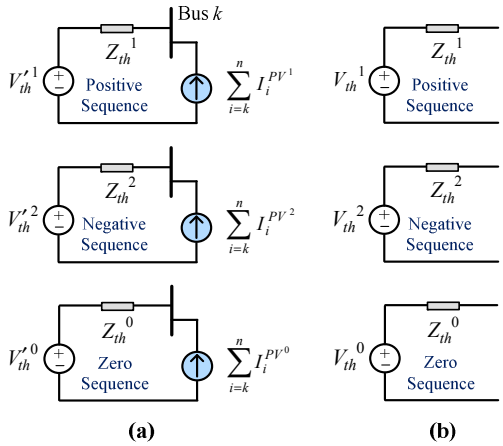

Fig. 3. Simplified equivalent sequence networks.

$$I_{no}{}^1 = \sum_{i=k}^{n} I_i^{PV^1}, \quad I_{no}{}^2 = \sum_{i=k}^{n} I_i^{PV^2}, \quad I_{no}{}^0 = \sum_{i=k}^{n} I_i^{PV^0} \tag{7}$$

where the suffix *no* denotes Norton equivalent. For the upstream PVs, the Thevenin equivalent is expressed as (8) where the suffix *th* denotes Thevenin equivalent. Simplifying the downstream Norton equivalent of (7) and upstream Thevenin equivalent of (8), can be expressed as (9) which is shown schematically in Fig. 3. Eq. (9) demonstrates that, in addition to expected negative and zero sequence impedance, a negative and zero sequence voltage also exists due to the presence of single–phase PVs distributed unequally among the three phases.

$$\begin{aligned} V'_{th}{}^1 &= 1 + \sum_{i=1}^{k-1} I_i^{PV^1}\left(Z_f^{MV^1} + Z^{trans^1} + iZ_f^{LV^1}\right) \\ V'_{th}{}^2 &= \sum_{i=1}^{k-1} I_i^{PV^2}\left(Z_f^{MV^2} + Z^{trans^2} + iZ_f^{LV^2}\right) \\ V'_{th}{}^0 &= \sum_{i=1}^{k-1} I_i^{PV^0}\left(Z^{trans^0} + iZ_f^{LV^0}\right) \end{aligned} \tag{8}$$

$$Z_{th}{}^{1} = Z_f^{MV^1} + Z^{trans^1} + kZ_f^{LV^1}$$

$$Z_{th}{}^{2} = Z_{th}{}^{1} \quad , \quad Z_{th}{}^{0} = Z^{trans^0} + kZ_f^{LV^0}$$

$$[\boldsymbol{V}_{th}]_{012} = [\boldsymbol{V}'_{th}]_{012} + \sum_{i=k}^{n} [\boldsymbol{I}_i^{PV}]_{012} [\boldsymbol{Z}_{th}]_{012} \tag{9}$$

B. Single–phase Ground Fault

Due to high probability of single–phase to ground faults, refereed as LG in this paper, only LG is focused in this research. For an LG, from the sequence network parameters of (9), the fault current is calculated from the sequence current components. Depending on the faulted phase, (i.e. Phase–A, B or C), the fault current at fault location is calculated as

$$[\boldsymbol{I}^{Fault}]_{ABC} = 3I[\lambda_A \quad \lambda_B a^2 \quad \lambda_C a]^T \tag{10}$$

$$\text{where } I = \frac{V_{th}{}^{1} + V_{th}{}^{2} + V_{th}{}^{0}}{Z_{th}{}^{1} + Z_{th}{}^{2} + Z_{th}{}^{0} + 3Z_{Fault}}$$

where Z_{Fault} is the fault impedance and $\lambda_j = 1$ if the LG fault is in phase j (j = A, B or C); otherwise it is zero.

After fault current calculation, the voltage across fault location in Fig. 3(b) is calculated using Kirchhoff's voltage rule in sequence components as

$$[\boldsymbol{V}_{Fault}]_{012} = [\boldsymbol{V}_{th}]_{012} - [\boldsymbol{I}]_{012} [\boldsymbol{Z}_{th}]_{012} \tag{11}$$

and is then transferred to phase components by

$$[\boldsymbol{V}_{Fault}]_{ABC} = [\boldsymbol{A}]_{012} [\boldsymbol{V}_{Fault}]_{012} \tag{12}$$

Later, Kirchhoff's voltage rule is used to calculate the voltage at each bus of the feeder in Fig. 1, in phase components.

C. Sensitivity Analysis

To investigate the effect of one single–phase rooftop PV on the network during an LG, a sensitivity analysis is required. The variables considered in the sensitivity analysis are PV rating and location as well as fault location. In this study, a discrete sensitivity analysis is carried out as the PV ratings are assumed to be varied from 0.7 to 3.5 kW in steps of 0.7 kW, the fault and PV locations are varied from bus 1 to bus n = 10 in steps of 1. The outputs of this analysis are the fault current, the current in transformer secondary and the voltage at each bus along the LV feeder. The results of this analysis are discussed in Section III.

D. Stochastic Analysis

A deterministic analysis may not be suitable due to the randomness in PV rating and location and the fault location [18]. Therefore, a stochastic analysis based on Monte Carlo method is carried out in this paper to investigate and predict the network parameters in case of an LG. The considered uncertainties in this research are: PV location and rating, penetration level of PVs in the network, and the fault location. The considered outputs of this analysis are the fault current and the voltage at each bus along the feeder. The flowchart of the developed Monte Carlo method is shown in Fig. 4.

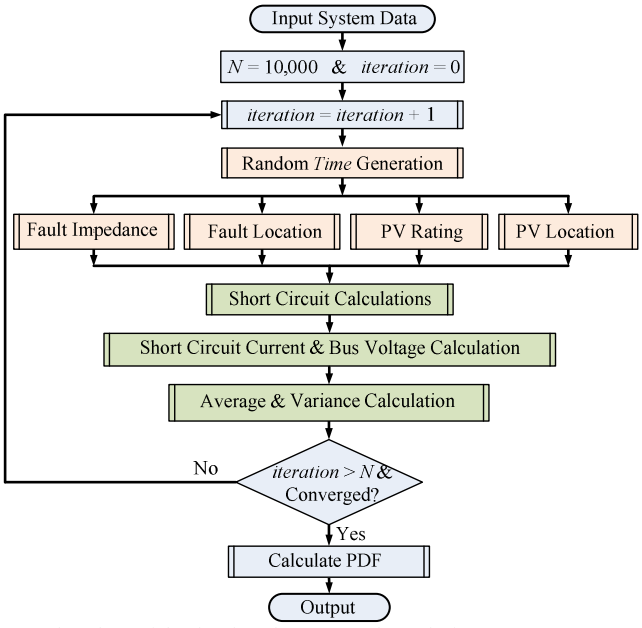

Fig. 4. Flowchart of the developed Monte Carlo analysis.

For reducing and eliminating the non–desired combinations of the variables for the stochastic analysis, a *Time* parameter is considered which represents the time of the analysis over the 24–hr period and is normalized in [0 1] range. *Time* is utilised to select correlated random values for the instantaneous output current available from PVs while the other variables are considered independent from *Time*. Only PV location and PV rating are assumed to have discrete values while the other variables are considered continuous. The output power of the PVs is assumed to have a normal distribution with an average of 2.5 and variance of 0.8 kW. PV installation point and fault location are assumed to have a uniformly distributed probability over 0–400 m range. Fault impedance is also assumed to have a uniform distribution over 0–0.3 ohm.

The stopping rule of the Monte Carlo method is chosen based on achieving an acceptable convergence for the average and variance of the desired outputs (i.e. short circuit current at fault location and bus voltages along the feeder). For this, the Monte Carlo simulation is deemed to have converged when a confidence degree of 95% is achieved. However, a minimum of N = 10,000 trials is utilized to avoid premature convergence. Once the Monte Carlo method is converged, the Probability Density Function (PDF) is defined of all outputs.

III. Sensitivity Analysis Results

As discussed in Section II, a sensitivity analysis is carried out to investigate the effect of one single–phase PV on the fault current, the current in transformer secondary and the voltage at each bus in the feeder, during an LG on phase–A at all buses with $Z_{Fault} = 0$.

A. Bus Voltage

First, the sensitivity analysis is carried out for the PV and fault location. Let us consider the network of Fig. 1 without

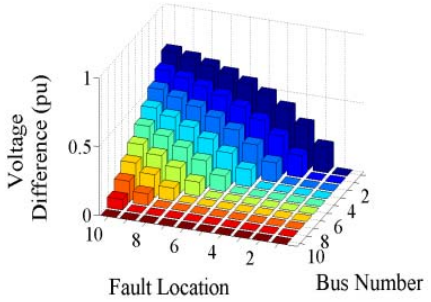

Fig. 5. Bus voltages in No–PV case.

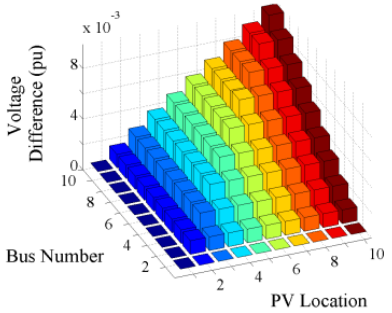

Fig. 6. Bus voltage difference for a fault in bus 1.

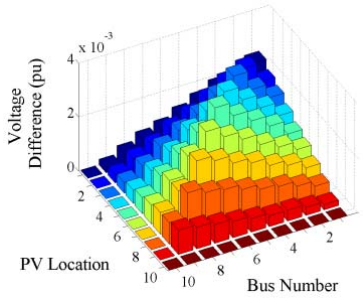

Fig. 7. Bus voltage difference for a fault in bus 10.

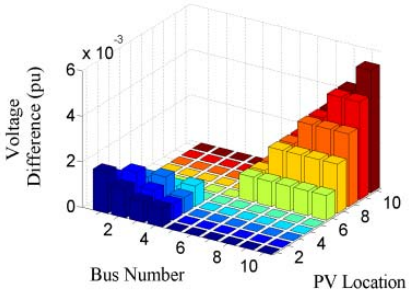

Fig. 8. Bus voltage difference for a fault in bus 5.

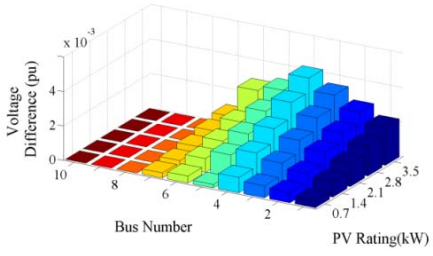

Fig. 9. Voltage difference.

any PVs (referred as No–PV case). In such a case, for the buses in upstream of the fault, the voltage decrease from transformer secondary towards the fault location but it is equal to zero for the buses in downstream of fault (Fig. 5).

Now, let us assume the LG is on phase–A at bus 1 (i.e. beginning of feeder) while a single–phase PV is located at different buses (i.e. bus 1 to 10) along the feeder (referred as PV–available case). The considered PV is assumed to have a nominal rating of 2 kW with a 150% current limiting, during fault. The results show that the voltage of the buses along the feeder in PV–available case is more than the No–PV case. This difference of bus voltages in two cases is shown in Fig. 6. This figure shows that the feeder end nodes always experience a higher voltage difference compared to feeder beginning nodes. Also it can be seen that, the voltage of the buses in upstream of PV location increase from feeder beginning towards PV location. However, this difference is not affected for the buses in the downstream of PV location. In addition, this voltage difference becomes higher as the PV is located in far end nodes of the feeder.

Now, let us assume the fault is in bus 10 (i.e. end of the feeder). In this case, the voltage difference is positive but is much smaller compared to the case when the fault is in bus 1 (Fig. 7). The voltage difference increases from the feeder beginning towards the PV location and then decreases towards the fault location. Note that the highest voltage difference is observed when the PV is located in the middle of the feeder.

Now, let us assume the fault is in bus 5 (i.e. middle of the feeder). The voltage difference has a similar trend to the one shown in Fig. 6 when the PV is located in upstream of the fault and a similar trend to the one shown in Fig. 7 when the PV is located in downstream of the fault (Fig. 8).

To investigate the effect of PV rating in short circuits, let us assume the LG is in bus 8 where a PV, located in bus 4, is assumed to have a rating of 0.7 to 3.5 kW, including the 150% current limiting. The voltage difference between the No–PV and PV–available cases is shown in Fig. 9. This figure shows that for higher PV ratings, larger voltage difference is observed.

B. Fault Current

The sensitivity analysis is repeated to investigate the PV effect on fault current and current in transformer secondary.

First, let us assume the PV has a nominal rating of 2 kW with a 150% current limiting. The PV and fault location are varied between bus 1 and 10. The fault current difference between the No–PV and PV–available modes as well as the difference of current in transformer secondary in these two cases are shown in Fig. 10(a) and (b), respectively.

Fig. 10(a) shows that by varying the fault location from beginning nodes of the feeder towards the end, the fault current difference increases when the PV is located in downstream of the fault and decreases when the PV is located in upstream of the fault. Note that when the PV is located in downstream of the fault, the PV location does not affect the fault current difference.

Fig. 10(b) shows the current in transformer secondary in the No–PV case is higher than the PV–available case. Hence, the difference values in Fig. 10(b) are all negative. This figure shows that when the PV is located in downstream of the fault, there is no difference between the transformer secondary current in No–PV and PV–available cases. It is also seen that as the PV is located closer to feeder beginning nodes, the transformer secondary current is much less than the No–PV case.

Now, let us assume the LG in bus 8 where a PV, located in bus 4, has a rating of 0.7 to 3.5 kW, including the 150% current limiting. The difference in the fault current between the No–PV and PV–available cases are shown in Fig. 11(a)

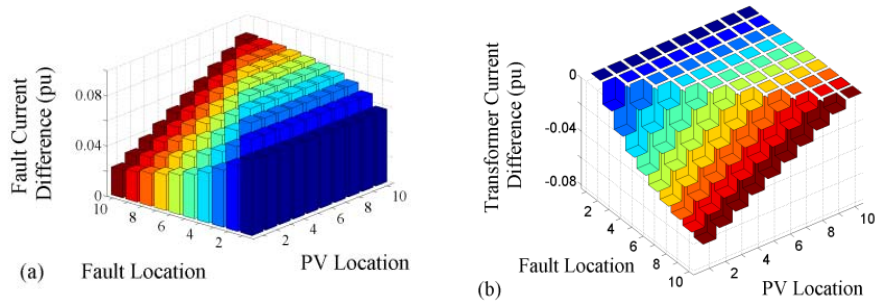

Fig. 10. Differenc in (a) fault current, (b) transformer secondary current.

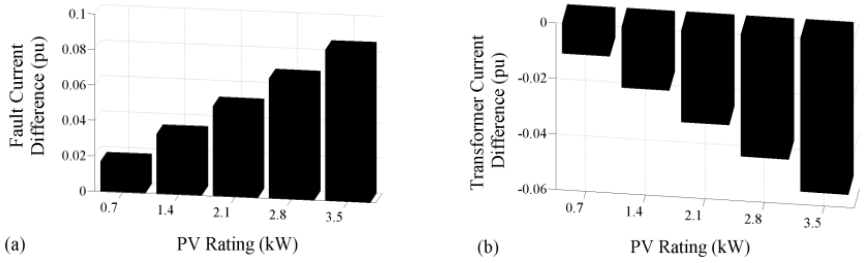

Fig. 11. PV rating effect on differenc in (a) fault current, (b) transformer secondary current.

while this difference for the current in transformer secondary is shown in Fig. 11(b). From these figures, it can be seen that, the fault current increases for higher PV ratings. In addition the reduction in current of transformer secondary is more for higher PV ratings.

IV. Stochastic Analysis Results

As discussed in Section II, a stochastic analysis is carried out to investigate the effect of multiple PVs at different locations and phases, different PV penetration levels and instantaneous output power of PVs during an LG. After the Monte Carlo method is converged, the PDF is defined and the average and variance of all iteration results for each output is recorded. In this study, the considered outputs are the current in transformer secondary and the voltage at each bus of feeder.

First, the Monte Carlo analysis is carried out assuming a 50% penetration level for the PVs while all the PVs have the same rating. Note that, depending on the parameter *Time*, the instantaneous output of PVs is different in Monte Carlo iterations. The results of this analysis are given in Table I. This table shows that the expected average voltage at each bus is not affected significantly by the PV ratings.

Then, another Monte Carlo analysis is carried out assuming all PVs have a rating of 2 kW with a 150% current limiting while different PV penetration levels are considered. The results of this analysis are given in Table II. This table shows that the expected average voltage at each bus is not also affected significantly by the increase in the PVs penetration level in the network.

Both of the previously discussed Monte Carlo analyses are repeated to investigate the expected PDF characteristics of the current in transformer secondary during the LG. The results of these analyses are given in Table III. These results show that different PV ratings and different PV penetration levels do not modify the expected current in transformer secondary during an LG.

Table I. Monte Carlo results for bus voltages (pu) for different PV ratings.

PV [kw]	V_1		V_5		V_{10}	
	mean	*std*	*mean*	*std*	*mean*	*std*
0.7	0.748	0.1742	0.557	0.2236	0.486	0.2513
1.4	0.749	0.1739	0.560	0.2239	0.490	0.2525
2.1	0.751	0.1736	0.563	0.2247	0.493	0.2537
2.8	0.754	0.1746	0.567	0.2255	0.496	0.2543
3.5	0.756	0.1751	0.570	0.2247	0.499	0.2539

Table II. Monte Carlo results for bus voltages (pu) for PV penetration levels.

Penetration [%]	V_1		V_5		V_{10}	
	mean	*std*	*mean*	*std*	*mean*	*std*
20	0.748	0.1733	0.558	0.2229	0.488	0.2518
40	0.749	0.1745	0.561	0.2242	0.490	0.2516
60	0.750	0.1760	0.561	0.2253	0.489	0.2536
80	0.755	0.1746	0.569	0.2258	0.497	0.2549
100	0.758	0.1763	0.571	0.2265	0.501	0.2552

Table III. Monte Carlo results for current in transformer secondary (pu).

PV [kw]	Current		Penetration [%]	Current	
	mean	*std*		*mean*	*std*
0.7	6.9221	2.9889	20	6.9381	2.9984
1.4	6.9364	2.9944	40	6.9336	2.9804
2.1	6.9421	2.9819	60	6.9490	2.9949
2.8	6.9227	3.0054	80	6.9040	3.0230
3.5	6.9328	3.0312	100	6.9050	3.0412

V. Conclusion

The effect of single–phase rooftop PVs was studied during a single–phase fault to ground fault in the residential low voltage overhead lines, for their contribution on the fault cur rent and the voltage at different buses along the feeder. The study was carried out by sensitivity and stochastic analyses.

The results of the sensitivity analysis demonstrated that the fault current is always higher in the presence of a PV in the feeder. The voltage of the buses along the feeder is dependent on the fault location and PV location. The voltage of the buses in the feeder in the presence of a PV is always higher than the case without the PV. This voltage difference is larger if the fault is closer to the beginning nodes of the feeder. In addition, the current observed in the secondary of the distribu-

tion transformer during the fault is reduced when a PV is present in the network and this difference is larger when the fault is closer to the end of the feeder.

The stochastic analysis results demonstrated that the expected probability density function for the bus voltages and current in transformer secondary by considering the uncertainties in fault location and impedance, PV location, rating, instantaneous output power and penetration level. The results of this analysis show that higher PV penetration level and higher PV ratings, do not affect significantly the probability density function of the bus voltages and transformer current.

REFERENCES

[1] M.A. Eltawil and Z. Zhao, "Grid–connected photovoltaic power systems: Technical and potential problems–A review," *Renewable & Sustainable Energy Reviews*, Vol. 14, pp.112–129, 2010.

[2] S.A. Papathanassiou, "A technical evaluation framework for the connection of DG to the distribution network," *Electric Power System Research*, Vol. 77, Issue 1, pp. 24–34, 2007.

[3] F. Shahnia, R. Majumder, A. Ghosh, G. Ledwich and F. Zare, "Voltage imbalance analysis in residential low voltage distribution networks with rooftop PVs," *Electric Power Systems Research*, Vol. 81, Issue 9, pp. 1805–1814, 2011.

[4] F. Shahnia, R. Majumder, A. Ghosh, G. Ledwich and F. Zare, "Voltage unbalance improvement in low voltage residential feeders with rooftop PVs using custom power devices," *International Journal of Electrical Power & Energy Systems*, Vol. 55, pp. 362–377, Feb. 2014.

[5] G. Mokhtari, A. Ghosh, G. Nourbakhsh and G. Ledwich, "Smart robust resources control in LV network to deal with voltage rise issue," *IEEE Trans. on Sustainable Energy*, Vol. 4, No. 4, pp. 1043–1050, Oct. 2013.

[6] V. Calderaro, S. Corsi, V. Galdi and A. Piccolo, "Optimal setting of the protection systems in distribution networks in presence of distributed generation," 40th Int. Universities Power Engineering Conf., Sept. 2005.

[7] T. Shun, G. Jing, X. Xiangning and L. Gang, "Influence analysis of DG penetration levels and grid–connected positions on traditional current protection," IEEE Electrical Power & Energy Conference (EPEC), 2011.

[8] H. Ravindra, M.O. Faruqe, P. McLaren, et al "Impact of PV on distribution protection system," North American Power Symposium, 2012.

[9] K. Kauheniemi and L. Kumpulainen, "Impact of distributed generation on the protection of distribution networks", 8th IEE Int. Conf. on Developments in Power System Protection, Vol. 1, pp. 315–318, April 2004.

[10] M.T. Doyle, "Reviewing the impact of distributed generation on distribution system protection," IEEE Power Engineering Society Summer Meeting, Vol. 1, pp. 103–105, 2002.

[11] K. Maki, S. Repo and P. Jarventausta, "Protection planning development for DG installations," 20th Int. Conf. on Electricity Distribution, 2009.

[12] IEEE Std. 1547.7– Guide to conducting distribution impact studies for distributed resource interconnection, 2012.

[13] R.A. Walling, R. Saint, R.C. Dugan, et al, "Summary of distributed resources impact on power delivery systems," *IEEE Trans. on Power Delivery*, Vol. 23, Issue 3, pp. 1636–1644, July 2008.

[14] S.A. Javidan, M.Haghifam," Implementation of a new protection scheme on a real distribution system in presence of DG," IEEE Power India Conference on Power System Technology (POWERCON), 2008.

[15] A.F. Viavan, D. Karlsson, A. Sannino, et al. "Protection scheme for meshed distribution systems with penetration of distributed generation," Power Systems Conference: Advanced Metering, Protection, Communication and Distributed Resources, March 2006.

[16] M. Mc Granaghan, T. Ortmeyer, D. Crudele, et al, "Advanced grid planning and operations," Sandia Technical Report, Feb. 2008.

[17] B. Subhashish, T. Saha and M.J. Hossein, "Fault current contribution from photovoltaic systems in residential power networks," Australian University Power Engineering Conf. (AUPEC), Tasmania, Oct. 2013.

[18] F. Shahnia, A. Ghosh, G. Ledwich and F. Zare, "Predicting voltage unbalance impacts of plug–in electric vehicles penetration in residential low voltage distribution networks," *Electric Power Components and Systems*, Vol. 41, Issue 16, pp. 1594–1616, Oct. 2013.